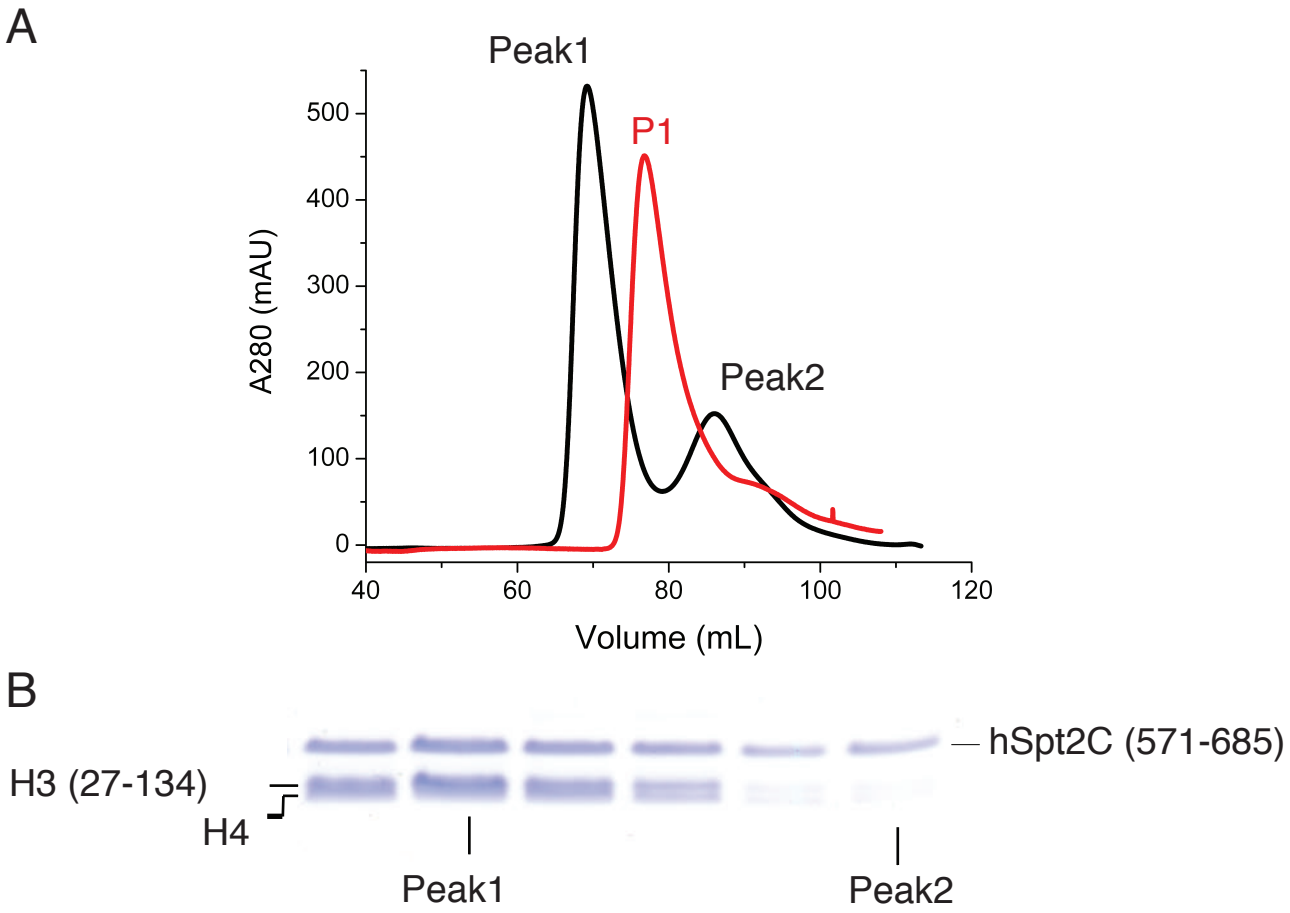

Supplemental Figure S1. Formation of complex of human hSpt2C bound specifically to Xenopus histone H3/H4 tetramer in high salt (2 M NaCl) solution. *(A)* Comigration of hSpt2C with histone H3/H4 tetramer in gel filtration assays. Red curve shows migration of histone H3/H4 tetramer, while black curve shows migration of complex. *(B)* Coomassie Blue staining of SDS-PAGE for complex peak (black curve) fractions in gel filtration assays. Peak 1 contains hSpt2C (571-685), H3 (27-134) and H4 proteins. Peak 2 represents excess hSpt2C protein.

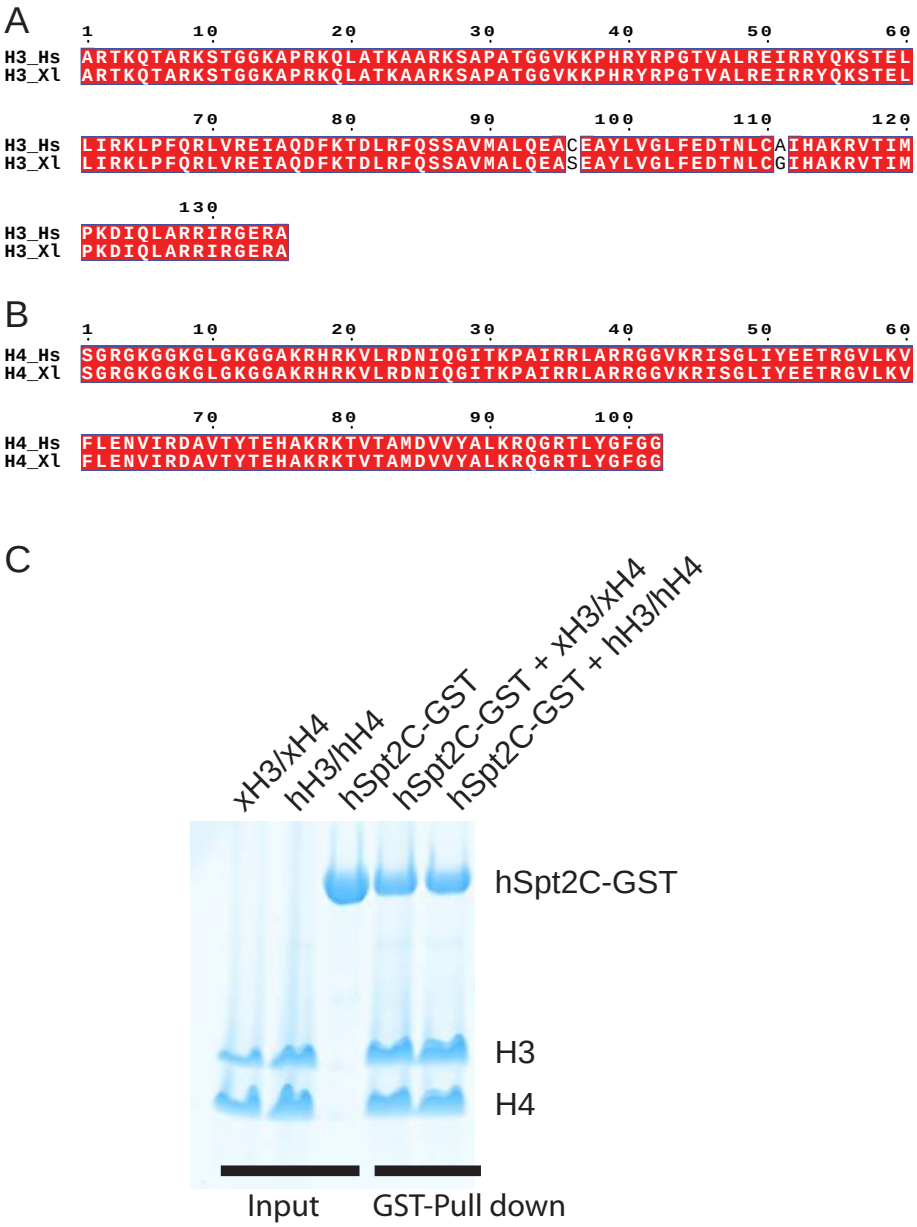

Supplemental Figure S2. Pull down assays for hSpt2C-GST with xenopus histone H3/H4 and human histone H3/H4. *(A)* Sequence alignment of human histone H3 (Hs) with xenopus histone H3 (Xl). *(B)* Sequence alignment of human histone H4 (Hs) with xenopus histone H4 (Xl). *(C)* GST-pull down assays of human Spt2C GST fusion protein with xenopus histone xH3/xH4 and human histone hH3/hH4.

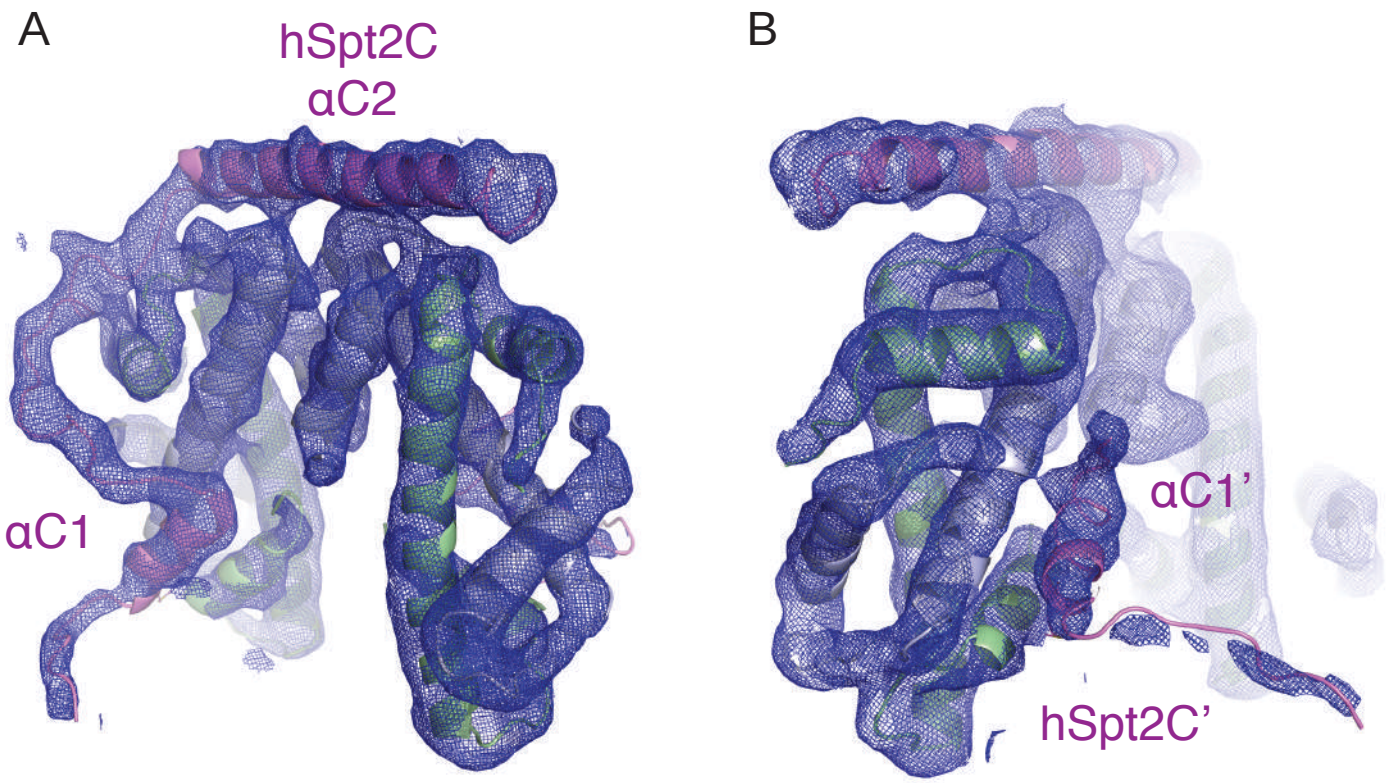

Supplemental Figure S3. Overall 2Fo-Fc maps (1.5σ level) between hSpt2C and the histone H3/H4 tetramer in the structure of the hSpt2C-H3/H4 tetramer complex. *(A)* Helix αC1 and αC2 are shown in first hSpt2C molecule. *(B)* Helix αC1' is shown in second hSpt2C molecule. Note that the second α helix is not connected to the first α helix in a different molecule in the crystal lattice.

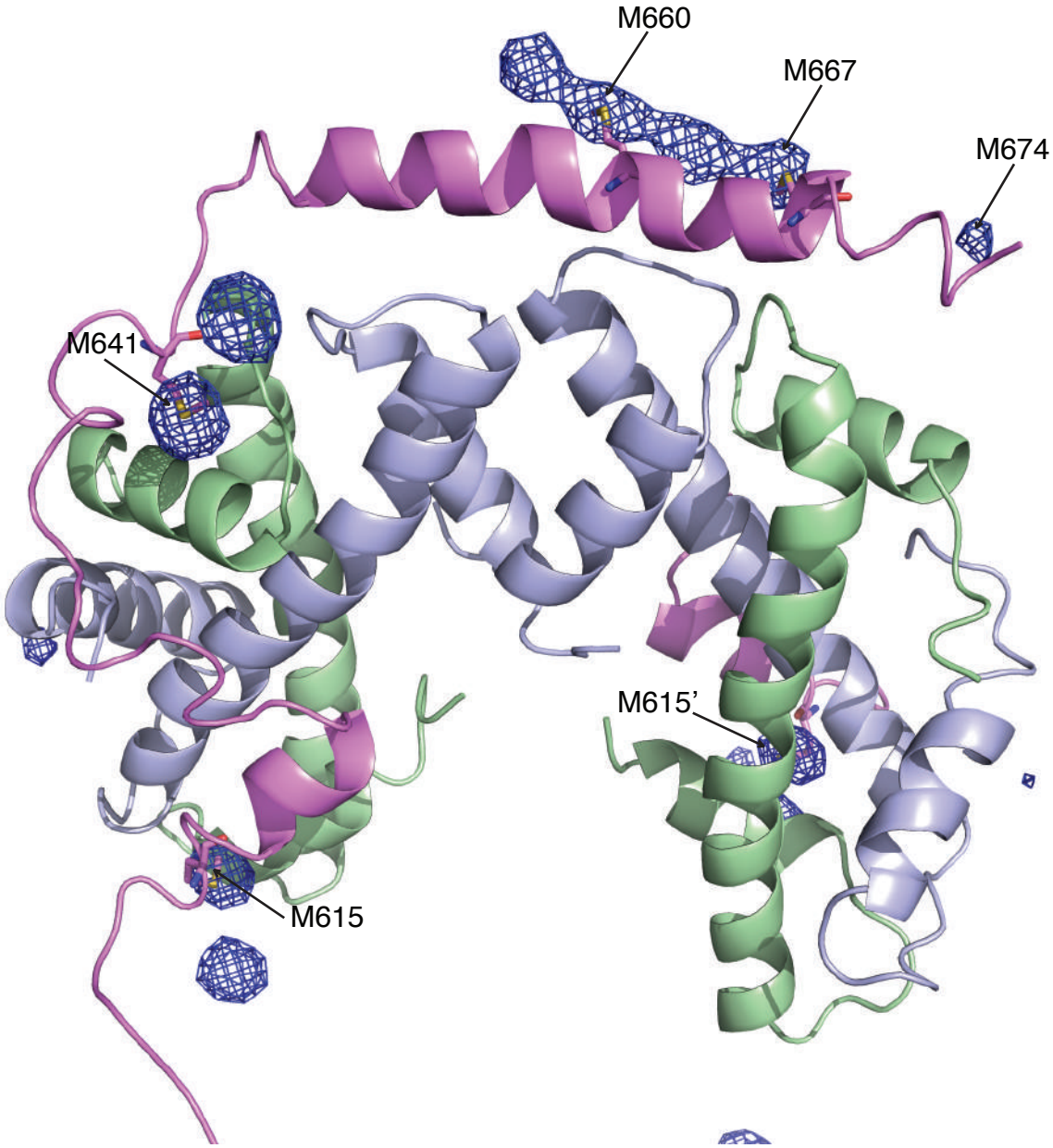

Supplemental Figure S4. Anomalous difference Fourier electron density map contoured at 5.0σ of selenomethionine substituted hSpt2C containing the I615M substitution in the hSptC2-H3/H4 tetramer complex identifying individual selenium positions (M615', M615, M641, M660, M667, M674) as shown surrounding the structure of the complex.

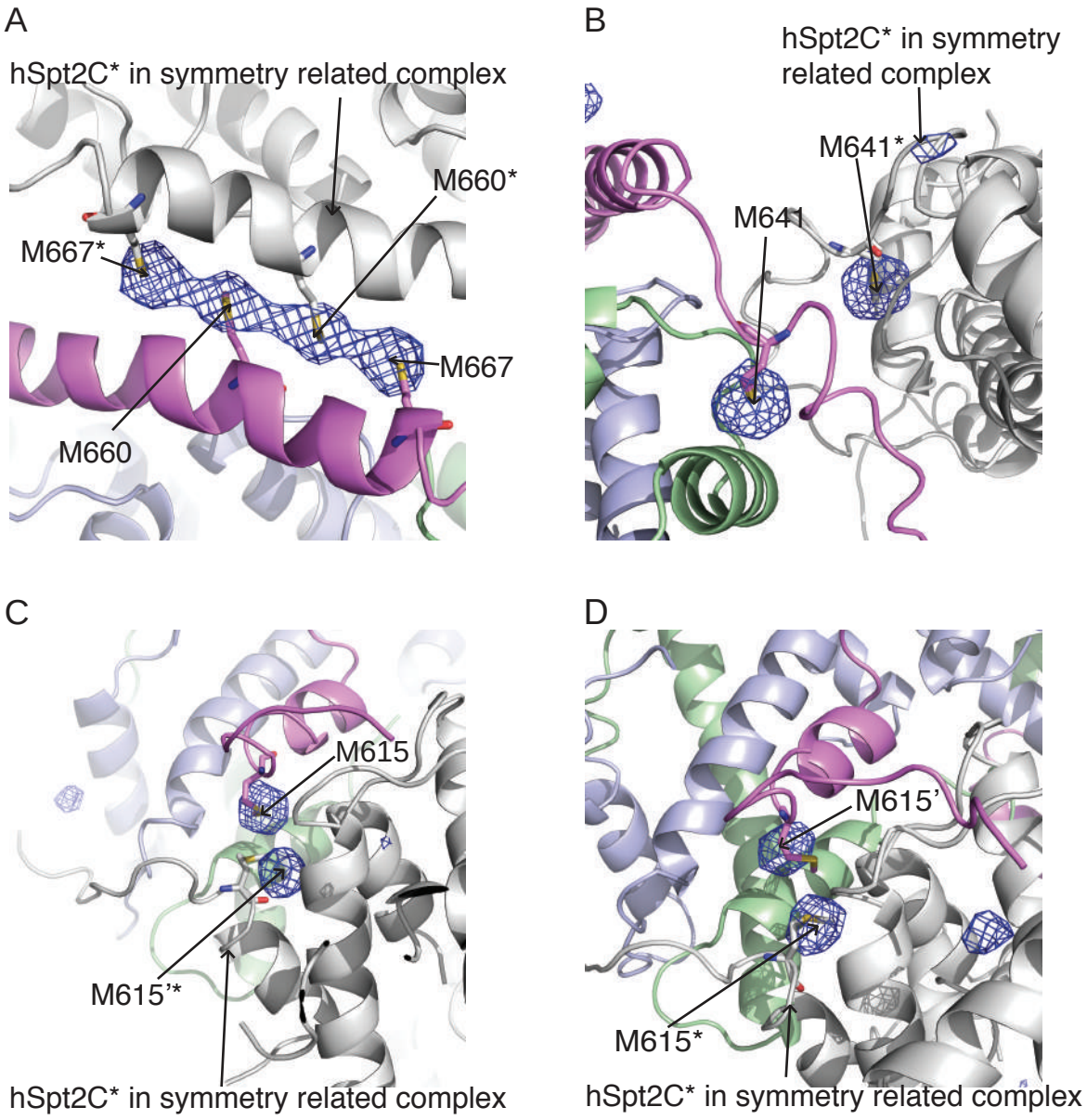

Supplemental Figure S5. Density related by 2-fold operation in the anomalous difference Fourier electron density map contoured at 5.0σ in the hSptC2(I615M,Se-Met)-H3/H4 tetramer complex, which originate from SeMet of hSpt2C in symmetry related complexes in the crystal lattice (panel *A* : M660, M667; panel *B*: M641; panel *C*: M615; panel *D*: M615'; residues from symmetry related complexes are labeled with star at the end). hSpt2C* is the long hSpt2C molecule and hSpt2C'* is the shorter hSpt2C molecule in symmetry related complexes in the crystal lattice.

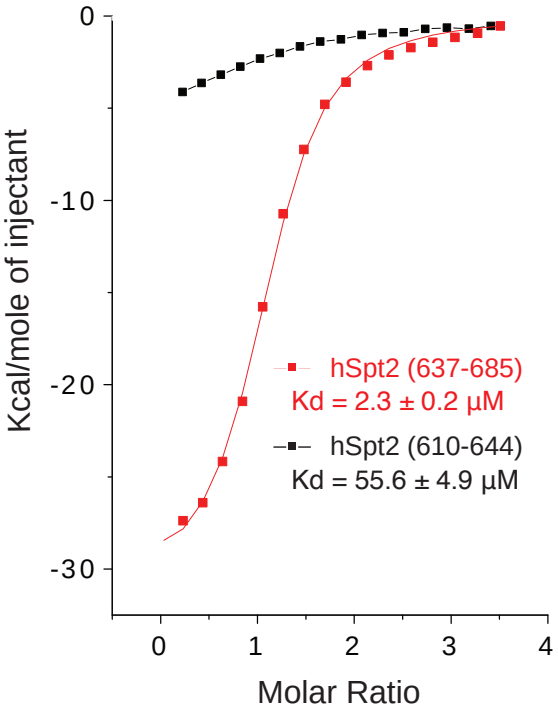

Supplemental Figure S6. ITC binding curve of hSpt2C fragments to H3/H4 in moderate salt (0.5 M NaCl) solution. Isothermal titration calorimetry (ITC) curves for binding of hSpt2C fragments to histone H3/H4 tetramer. hSpt2 (637-685) encompasses αC1 and αC2, while hSpt2 (610-644) encompasses αC1.

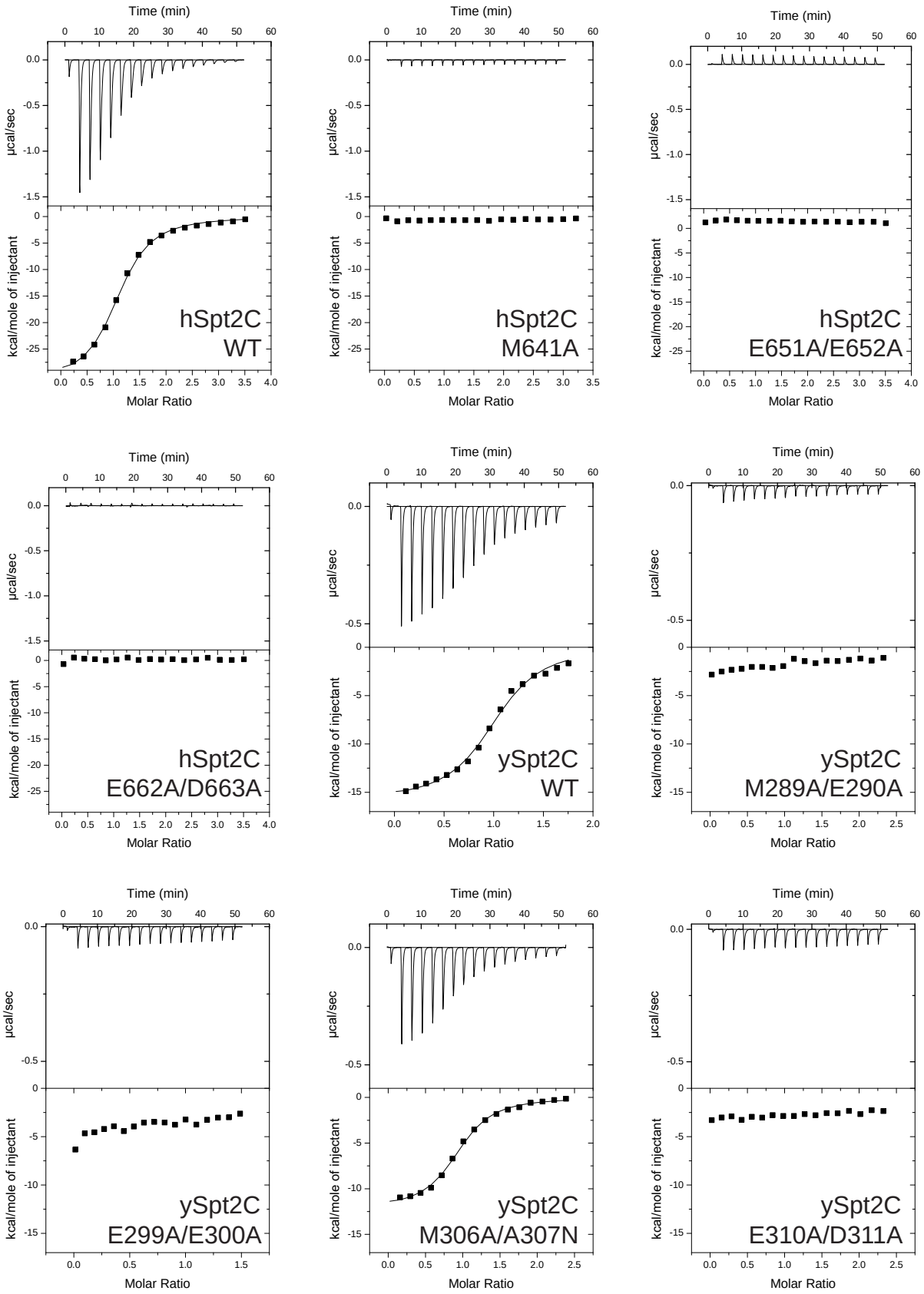

Supplemental Figure S7. Raw data of ITC assays. ITC-based binding parameters see supplementary Table S3.

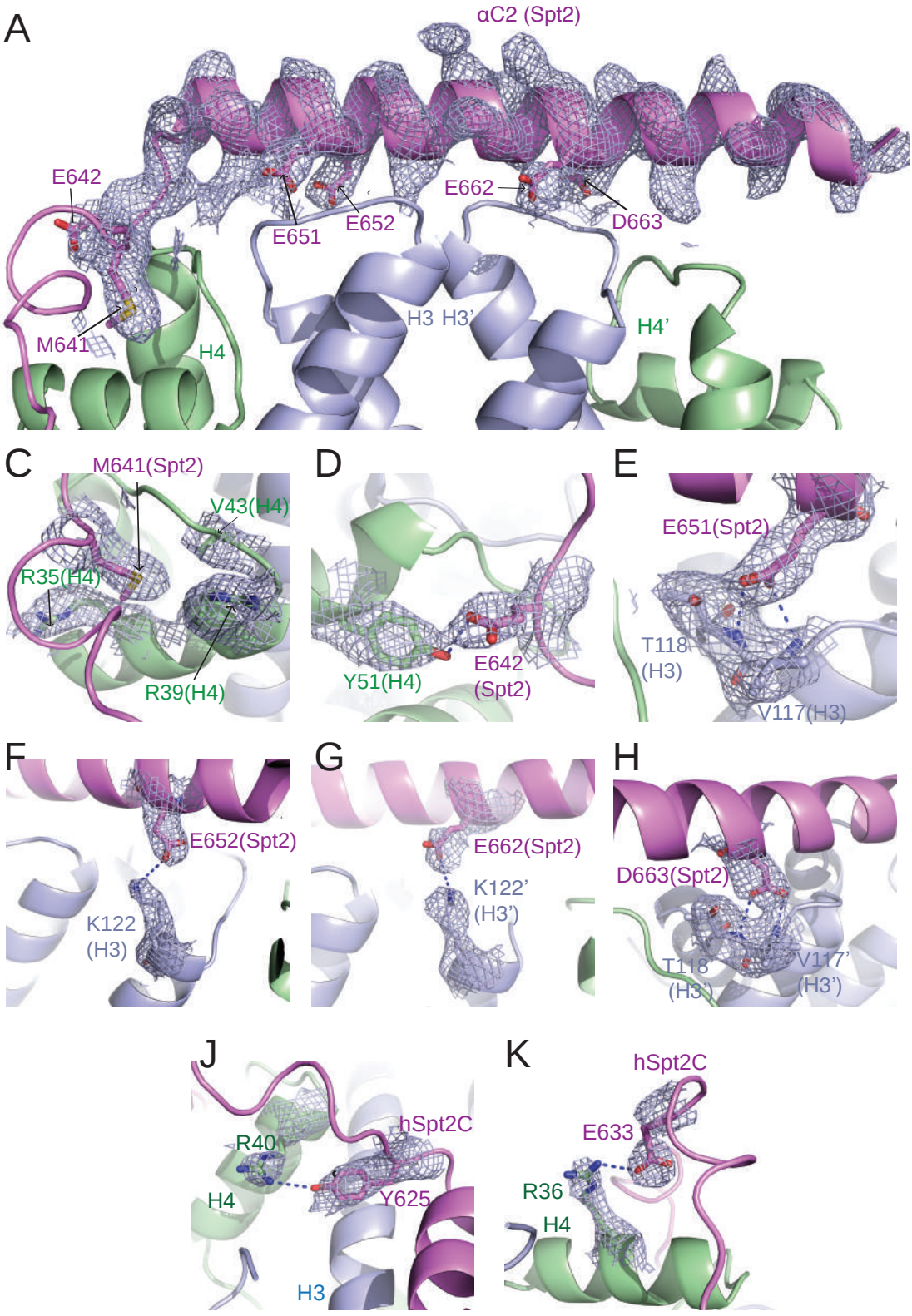

Supplemental Figure S8. 2Fo-Fc maps (1.2σ level) between hSpt2C and the histone H3/H4 tetramer in the structure of the hSpt2C-H3/H4 tetramer complex. *(A)* Overview of intermolecular contacts under consideration in the hSpt2C-H3/H4 tetramer complex. Expanded views labeled *C* to *K* are outlined below. *(C-K)* Intermolecular contacts between residue M641 (panel *C*) and E642 (panel *D*) of hSpt2C and residues within H4, between residues E651 (panel *E*) and E652 (panel *F*) of hSpt2C and residues within H3, between E662 (panel *G*) and D663 (panel *H*) of hSpt2C and residues positioned within H3, between Y625 (panel *J*) and E633 (panel *K*) of hSpt2C and residues within H4 in the complex. Hydrogen bonding are indicated by blue dashed lines and labeled with measured bond distances.

A

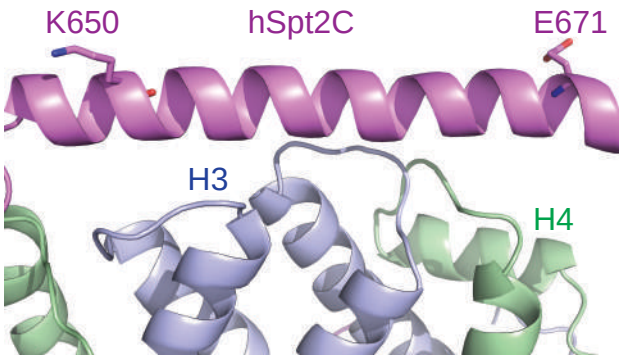

B

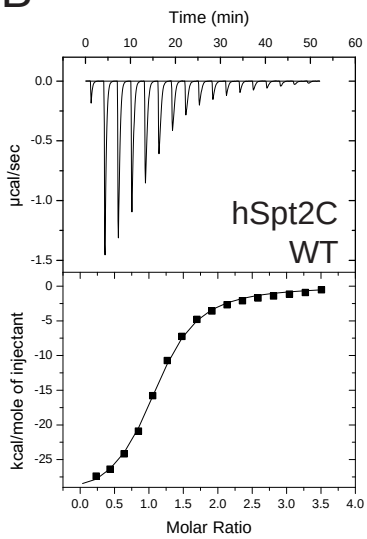

N 0.98 ± 0.01
Kd 2.3 ± 0.22 (µM)
ΔH -38.89 ± 0.49 (kcal/mol)
ΔS -109 (cal/mol/deg)

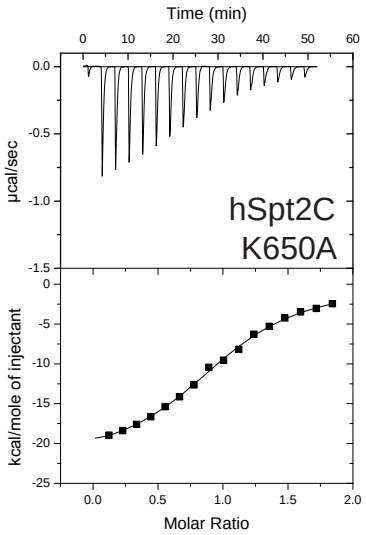

N 0.89 ± 0.01
Kd 6.4 ± 0.39 (µM)
ΔH -24.9 ± 0.3 (kcal/mol)
ΔS -61.2 (cal/mol/deg)

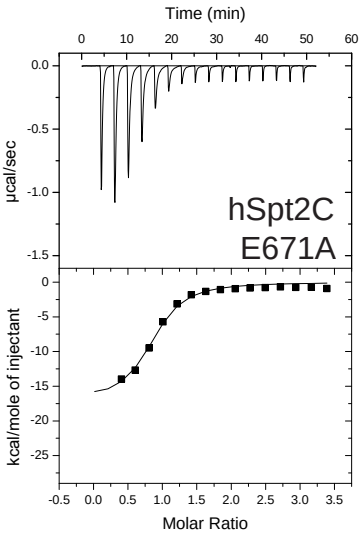

N 0.83 ± 0.03
Kd 4.1 ± 0.87 (µM)
ΔH -17.1 ± 0.97 (kcal/mol)
ΔS -33.6 (cal/mol/deg)

Supplemental Figure S9. Assays of non-histone contact residues mutant (K650A and E671A) of hSpt2C interacting with histone H3/H4. *(A)* Locations of K650 and E671 in hSpt2C. *(B)* ITC assays of non-histone contact residues mutants with histone H3/H4.

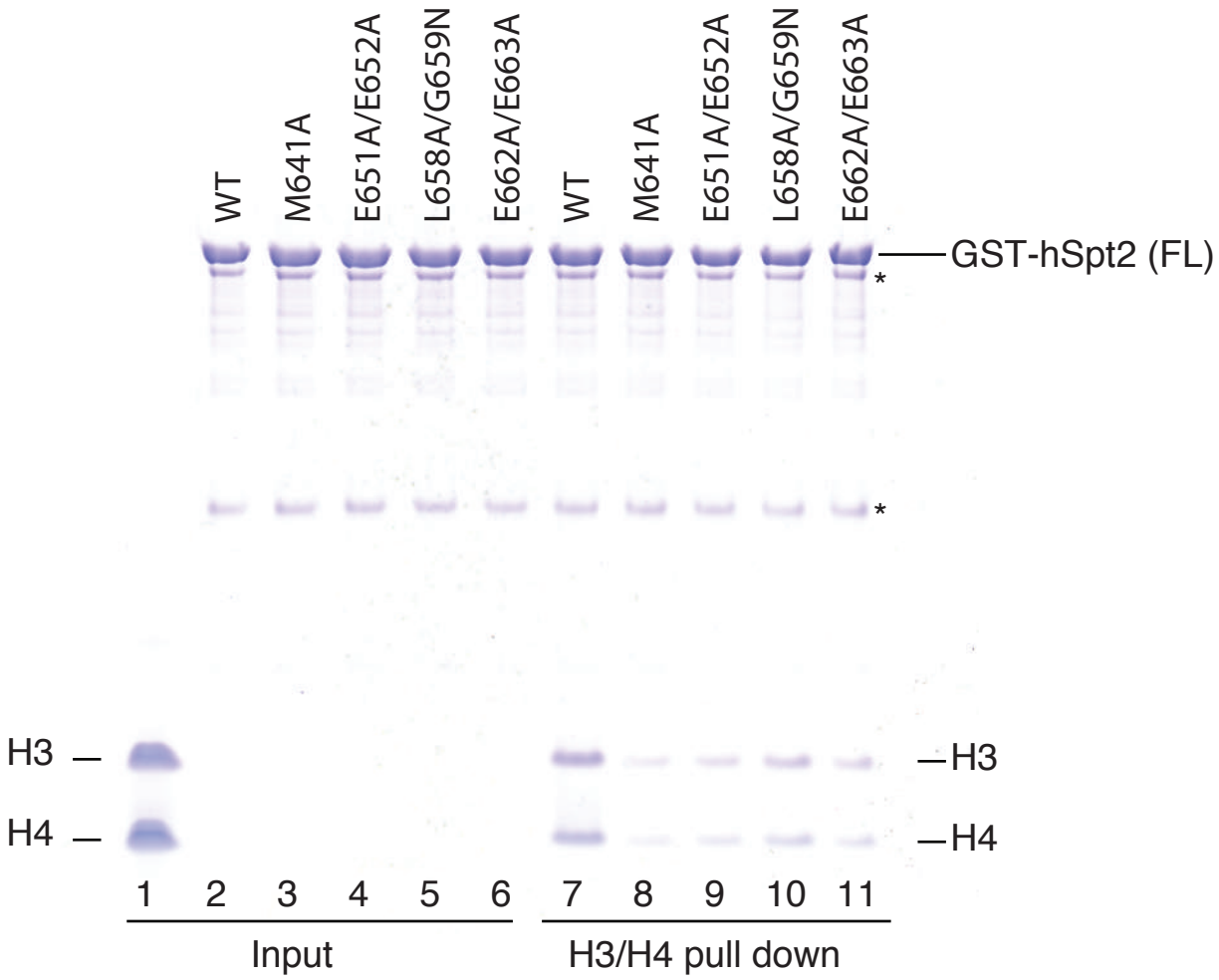

Supplemental Figure S10. Binding ability of wild-type and mutant full-length hSpt2 protein to histone H3/H4 tetramer in 0.7 M NaCl solution. In vitro pull-down assays for immobilized wild-type and mutants full-length human Spt2 binding to H3/H4 tetramer. Lanes 1: Input of H3/H4 tetramer. Lane 2-6: GST pull-down of wild-type or mutants full-length GST-hSpt2 protein without H3/H4 tetramer. Lanes 7-11: GST pull-down results of immobilized hSpt2 (wild-type or mutants) binding to H3/H4 tetramer in buffer 0.7 M NaCl, 10 mM Tris-HCl pH 7.5, 1 mM DTT. Asterisks indicate apparent degradation fragments of full-length GST-hSpt2.

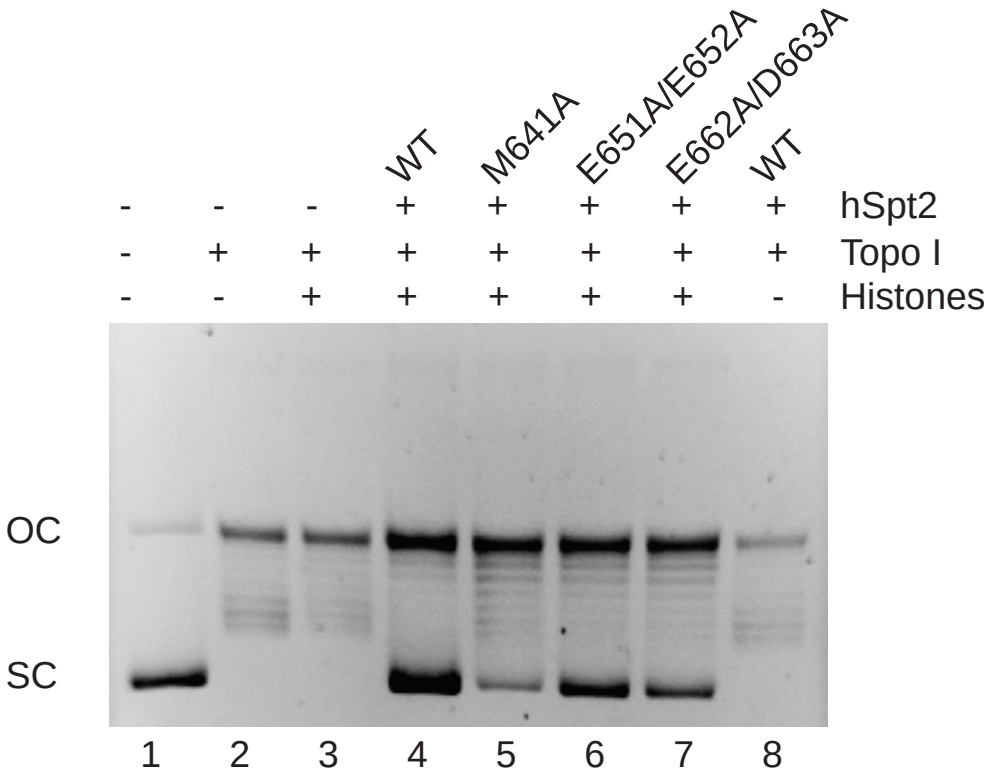

Supplemental Figure S11. Supercoiling assays for nucleosome assembly activity using wild-type and mutant hSpt2. Nucleosome assembly activity of wild-type hSpt2 and mutants indicate an important role of hSpt2-H3/H4 interaction in the deposition of histones. Lane 1: Supercoiling DNA template samples; Lane 2: Relaxed DNA treated with topoisomerase I; Lane 3: Sample containing relaxed DNA and histones, without hSpt2; Lane 4-7: Samples containing relaxed DNA and histone, in the present of wild-type hSpt2 or mutants. Lane 8: Samples containing relaxed DNA and wild-type hSpt2, without histones.

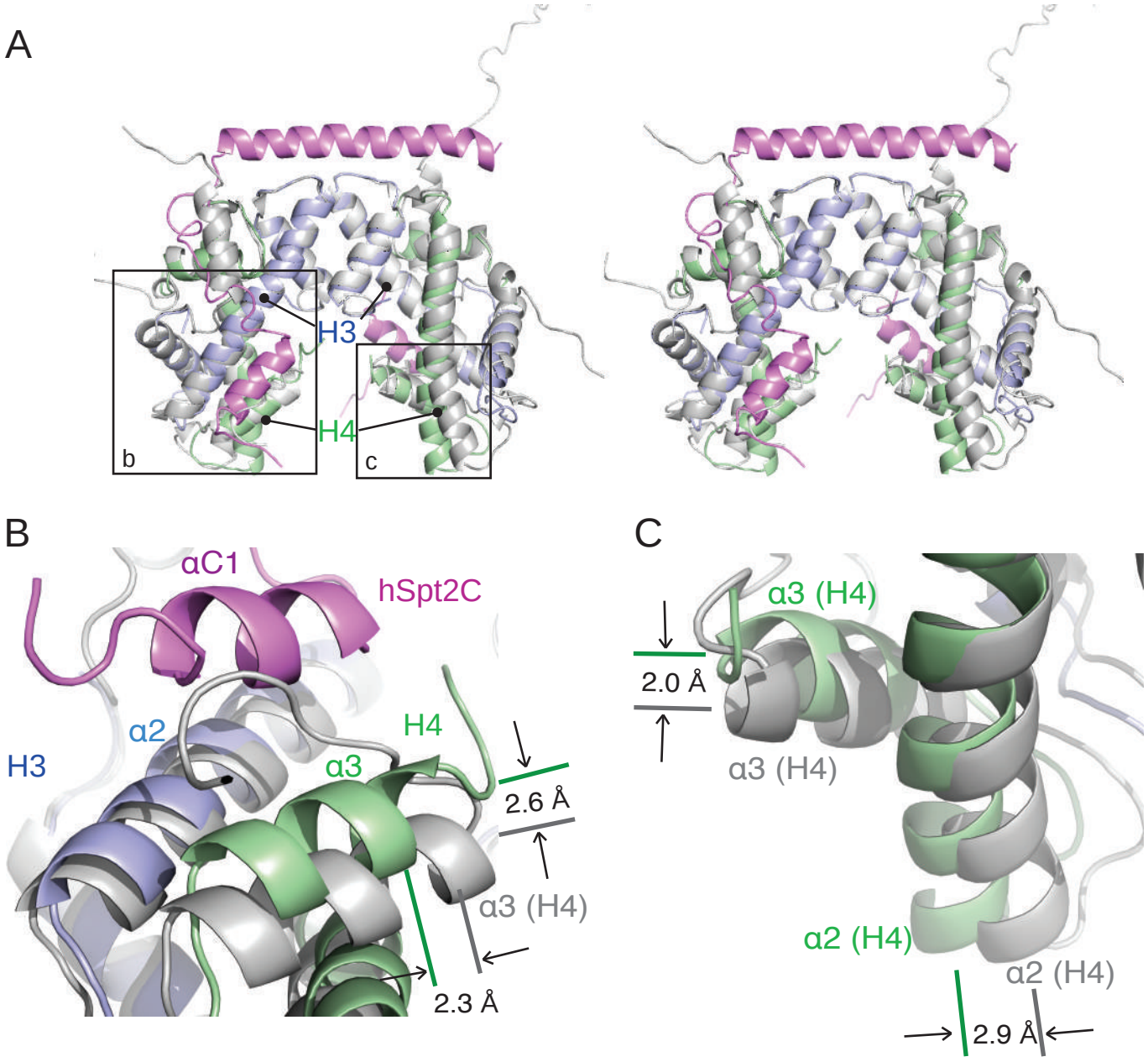

Supplemental Figure S12. Comparison of the structures of the H3/H4 tetramer in the hSpt2C-H3/H4 tetramer complex and mononucleosomes. *(A)* Stereo view of superposition of H3/H4 tetramer in the hSpt2C-H3/H4 tetramer complex (in color) with mononucleosomes (in silver; PDB code: 1AOI). *(B)* An expanded view highlighting differences in positioning of α3 of H4 between the two complexes. *(C)* An expanded view highlighting differences in positioning of α2 of H4 between the two complexes.

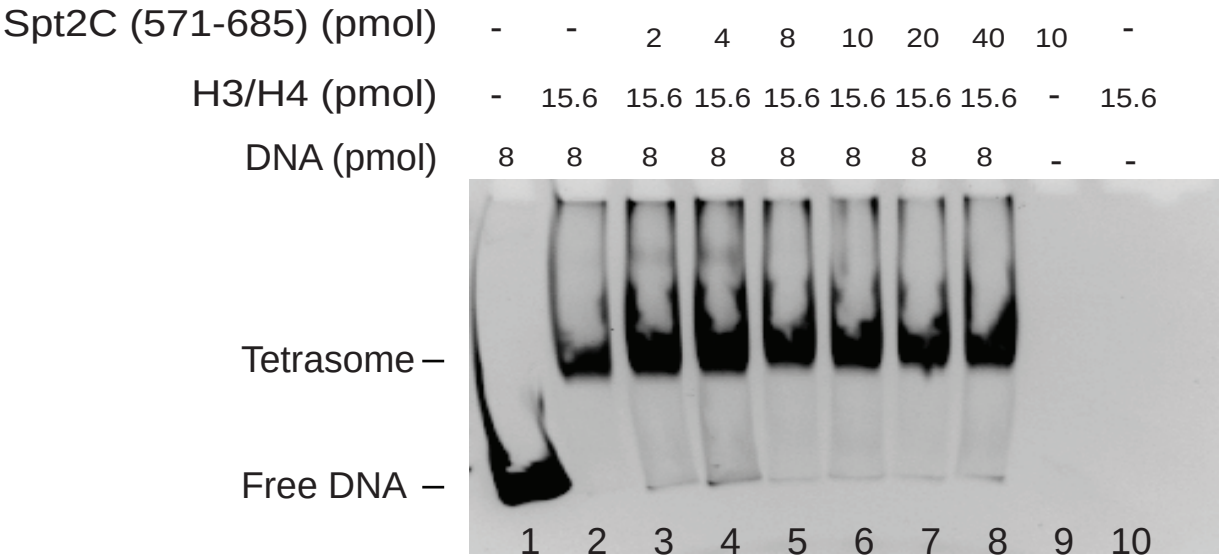

Supplemental Figure S13. Tetrasome assembly assays. Lane 1: Free DNA control; Lane 2: Tetrasome complex, containing DNA and histone H3/H4; Lane 3-8: Increasing amount of Spt2C protein in tetrasome solution; Lane 9: Spt2C protein control; Lane 10: Histone H3/H4 control.

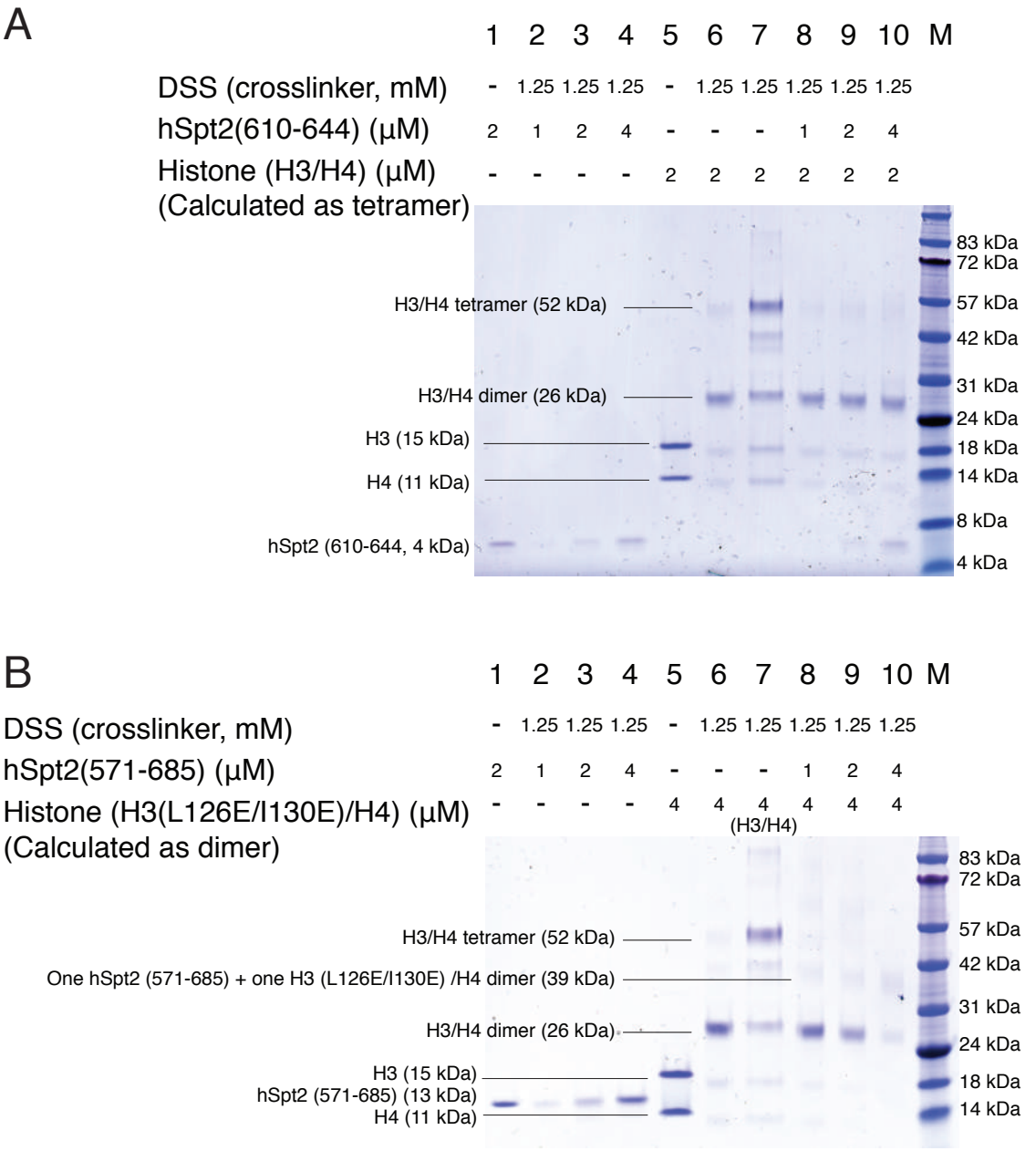

Supplemental Figure S14. Disuccinimidyl suberate (DSS)-mediated crosslinking assays of hSpt2(610-644) to histone H3/H4 tetramer and hSpt2C(571-685) to histone H3(L126E/I130E)/H4 dimer under physiological salt (0.15 M NaCl) condition. *(A)* DSS-crosslinking assays of hSpt2(610-644) to histone H3/H4 tetramer. Lanes 1: Input of hSpt2(610-644) protein. Lane 2-4: crosslinking of hSpt2(610-644) alone with indicated concentration. Lane 5: Input of histone H3/H4. Lanes 6: crosslinking of histone H3/H4 alone under 0.15 M NaCl salt condition. Lane 7: crosslinking of histone H3/H4 alone under 0.5 M NaCl salt condition. Lane 8-10: crosslinking of indicated concentration hSpt2(610-644) to histone H3/H4 under 0.15 M NaCl salt condition. Lane M: protein marker. *(B)* DSS-crosslinking assays of hSpt2(571-685) to histone H3(L126E/I130E)/H4 dimer. Lanes 1: Input of hSpt2(571-685) protein. Lane 2-4: crosslinking of hSpt2(571-685) alone with indicated concentration. Lane 5: Input of histone H3(L126E/I130E)/H4. Lanes 6: crosslinking of histone H3(L126E/I130E)/H4 alone under 0.15 M NaCl salt condition. Lane 7: crosslinking of wild-type histone H3/H4 alone under 0.5 M NaCl salt condition. Lane 8-10: crosslinking of indicated concentration hSpt2(571-685) to histone H3(L126E/I130E)/H4 under 0.15 M NaCl salt condition. Lane M: protein marker.

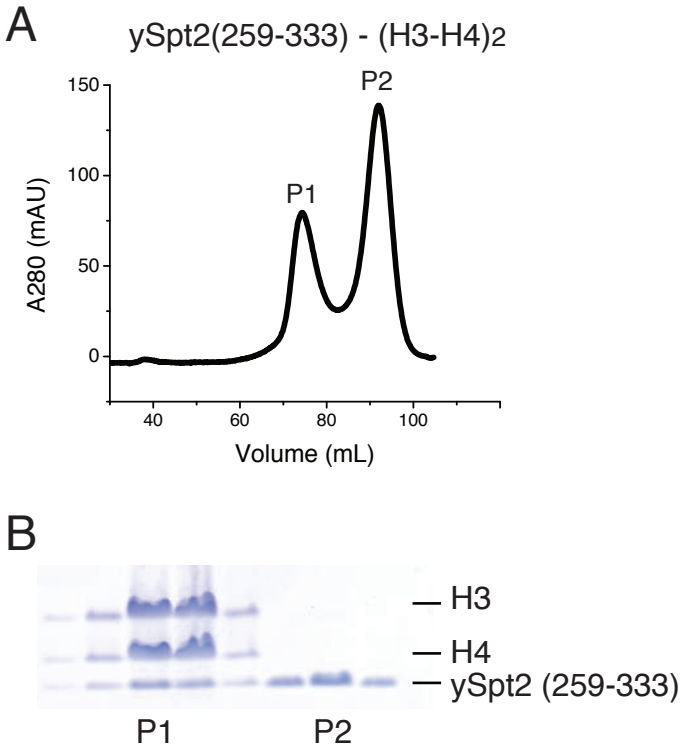

Supplemental Figure S15. Yeast ySpt2C bind specifically to histone H3/H4 tetramer under high salt (2.0 M NaCl) condition. *(A)* Comigration of ySpt2 (259-333) with histone H3/H4 tetramer during gel filtration. *(B)* Coomassie Blue staining of SDS-PAGE for identifying complex peak fractions in gel filtration assays. Peak labeled P1 contains ySpt2C (259-333), H3 and H4 proteins. Fraction peak labeled P2 contains excess ySpt2C (259-333).

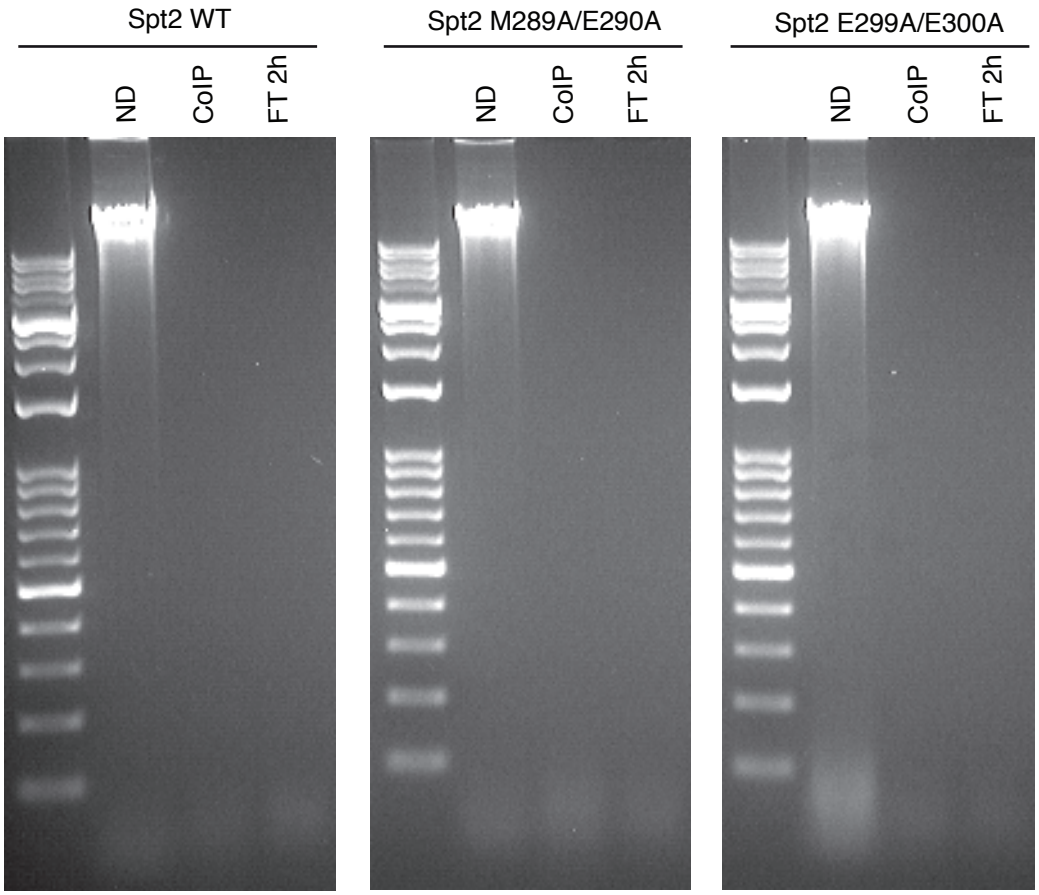

DNA control of Benzonase digestion: 200U 15min at RT

Supplemental Figure S16. Nuclease treatment of nuclear extracts used in Spt2-H3 co-immunoprecipitation experiments. After Benzonase treatment, DNA is undetected in the nuclear extracts. ND is for Non-Digested extracts, CoIP is for the digested extracts used in the indicated co-immunoprecipitation experiments and FT is for the Flow through after 2 hours binding to the beads.

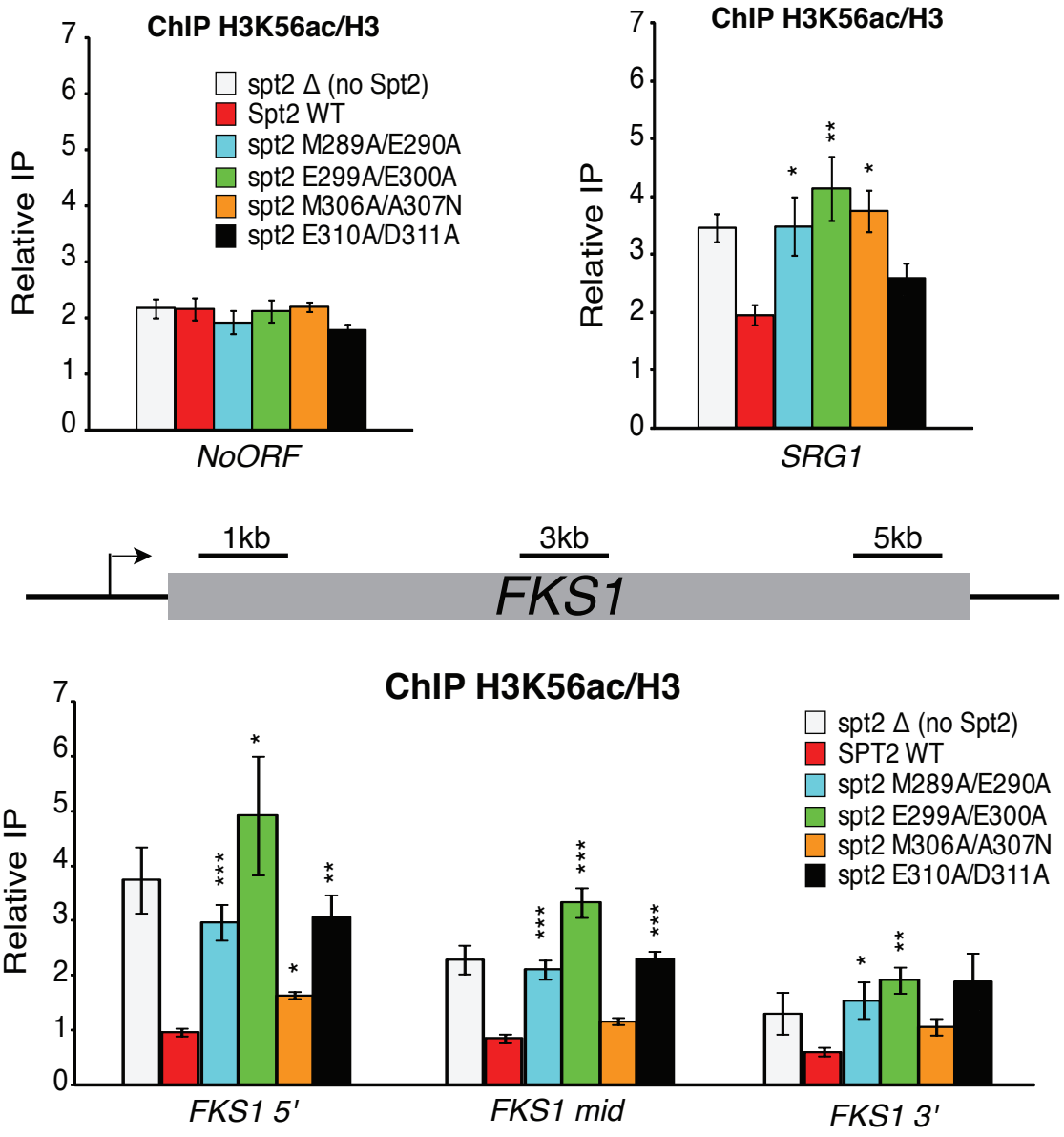

Supplemental Figure S17. Mutation of yeast Spt2 residues that are critical to the interaction with H3/H4 tetramer leads to a substantial increase in the level of H3K56ac at transcribed loci. Chromatin immunoprecipitations assessing H3K56 acetylation level in G1 arrested cells expressing different versions of Spt2. The non-transcribed intergenic region of chromosome V was tested along with the transcribed region of SRG1 and FKS1. Increased incorporation of H3K56ac mark suggests a higher exchange of H3/H4. These experiments were done in triplicates, one * indicates a p-value< 0.05, ** is for a p-value< 0.01 and *** is for a p-value< 0.001.

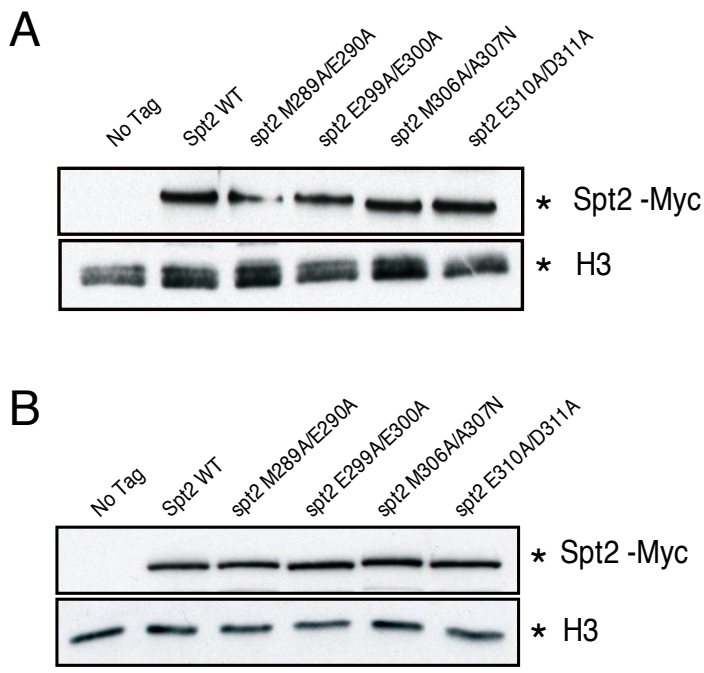

Supplemental Figure S18. In the H3K56ac ChIP assays and functional growth tests, the yeast Spt2 mutated forms are produced to the same level as wild type. *(A)* Western blot indicating that the levels of Spt2 protein containing mutations in critical H3/H4 interaction residues are similar to wild type Spt2. The proteins analyzed were extracted from cells that were used for ChIP assays shown in Figure 6. Cells containing the indicated version of Spt2 were grown to mid log phase and arrested in G1. After three hours of alpha factor treatment, the cells were harvested and the proteins were extracted. Total H3 level is used as a control. *(B)* Western blot indicating that the levels of Spt2 protein containing mutations in critical H3/H4 interaction residues are similar to wild type Spt2. The proteins analyzed were extracted from cells that were used in the growth assays shown in Figure 6. Cells containing the indicated version of Spt2 were grown to mid log phase in minimal media and either used in growth test (Fig. 6) or harvested to make protein extracts that were subsequently analyzed by anti-myc (Spt2) or anti-H3 western blotting.

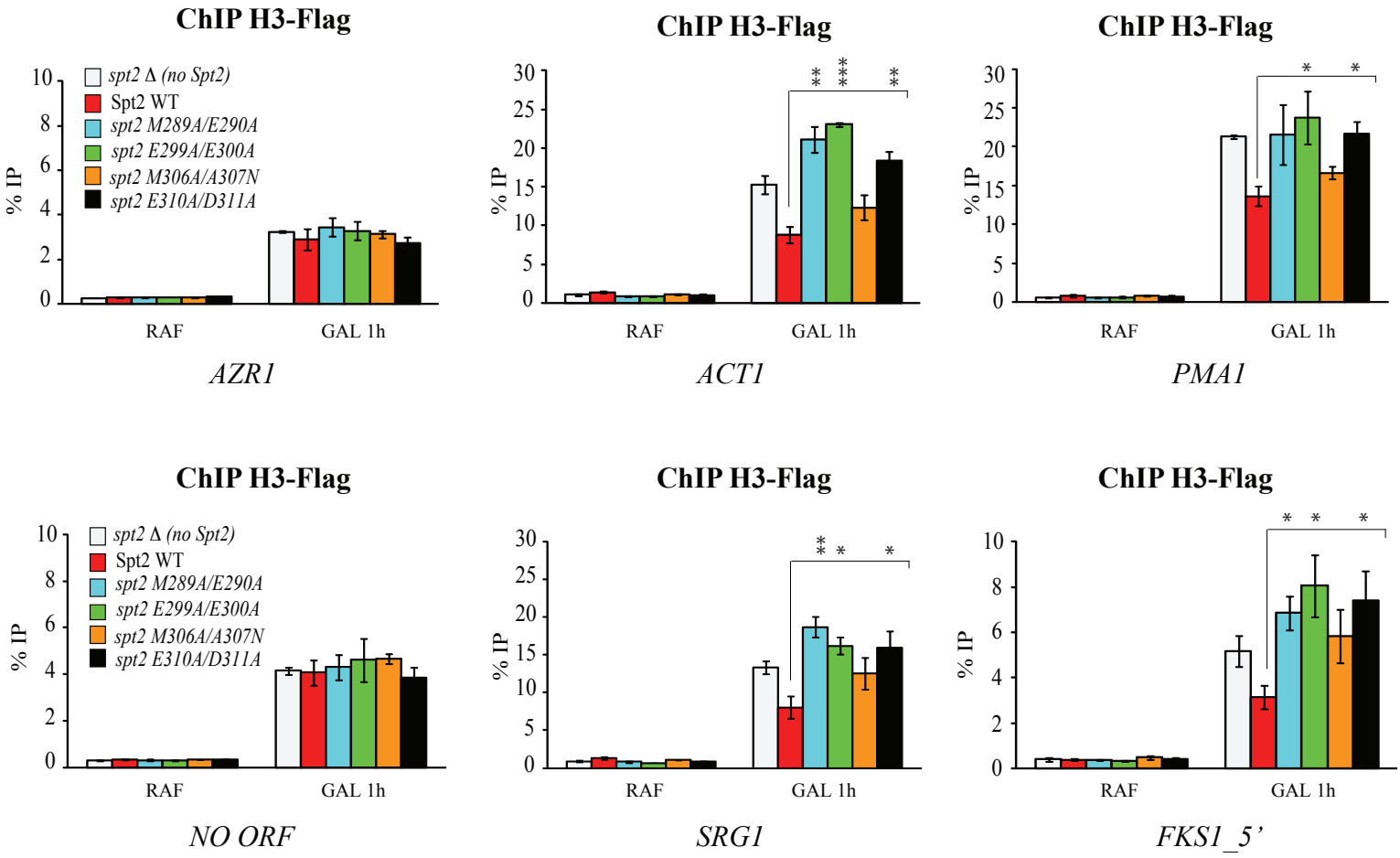

Supplemental Figure S19. Mutation of yeast Spt2 residues that are critical to the interaction with H3/H4 tetramer leads to a substantial increase in the incorporation of new H3. Chromatin immunoprecipitations assessing the incorporation of newly synthesized histone H3 at different locations. We used an experimental system described previously and based on the study of replication-independent histone H3 dynamics. In this system, there are two sources of histone H3, the endogenous untagged histone and a galactose-inducible form fused to the Flag tag. To eliminate the contribution of DNA replication-dependant histone deposition, the cells are blocked in G1 with α-factor. After that, cells are either fixed or induced to express Flag-H3 during 1 hour prior to formaldehyde treatment. Next, the level of Flag-H3 (trans-histones) and total H3 are assayed by standard ChIP-QPCR. Importantly, new H3 incorporation increases significantly at coding regions of active genes in spt2 mutants that are defective in the interaction with H3/H4. This indicates a crucial role of Spt2-H3/H4 interaction in the inhibition of H3/H4 exchange in transcribed loci. The values shown represent the ratio of new H3 divided by total H3 and indicate the replication-independent H3 exchange level in the regions tested. These experiments were done in triplicates, one * is for a p-value< 0.05, ** is for a p-value< 0.01 and *** is for a p-value< 0.001.

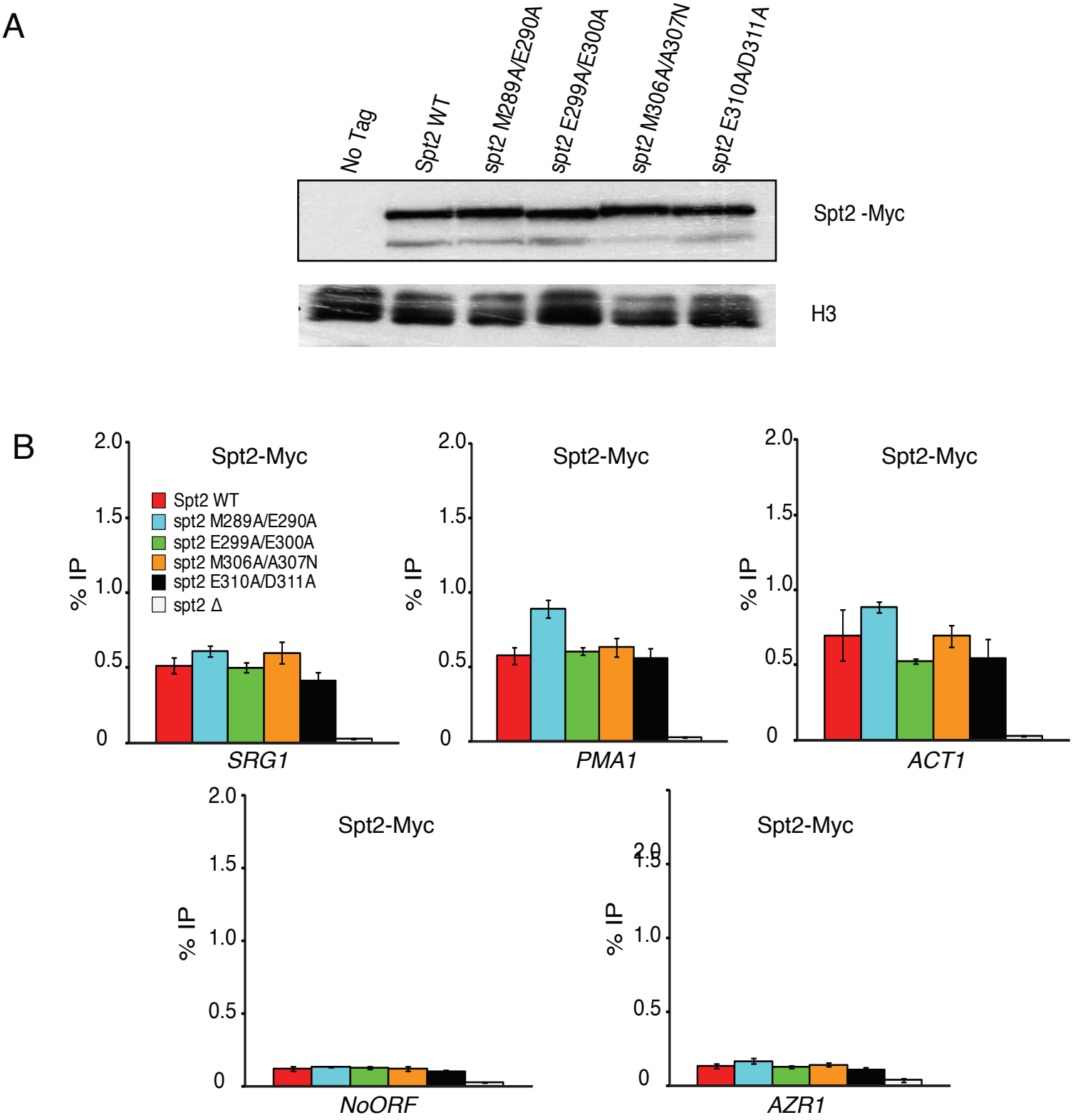

Supplemental Figure S20. The yeast Spt2 mutated in critical H3/H4 interaction residues are produced and recruited to coding regions of active genes. *(A)* Western blot indicating that the levels of Spt2 protein containing mutations in critical H3/H4 interaction residues are similar to wild type Spt2. Total H3 level is used as a control. *(B)* Chromatin immunoprecipitation assays analyzing the association of different yeast Spt2-Myc versions to coding regions of active (SRG1, PMA1 and ACT1) or inactive genes (AZR1 and NoORF (Intergenic Ch V)). Untagged yeast strain (spt2Δ) is used as control in the ChIP assays. The values shown represent the average and standard error of three independent experiments.

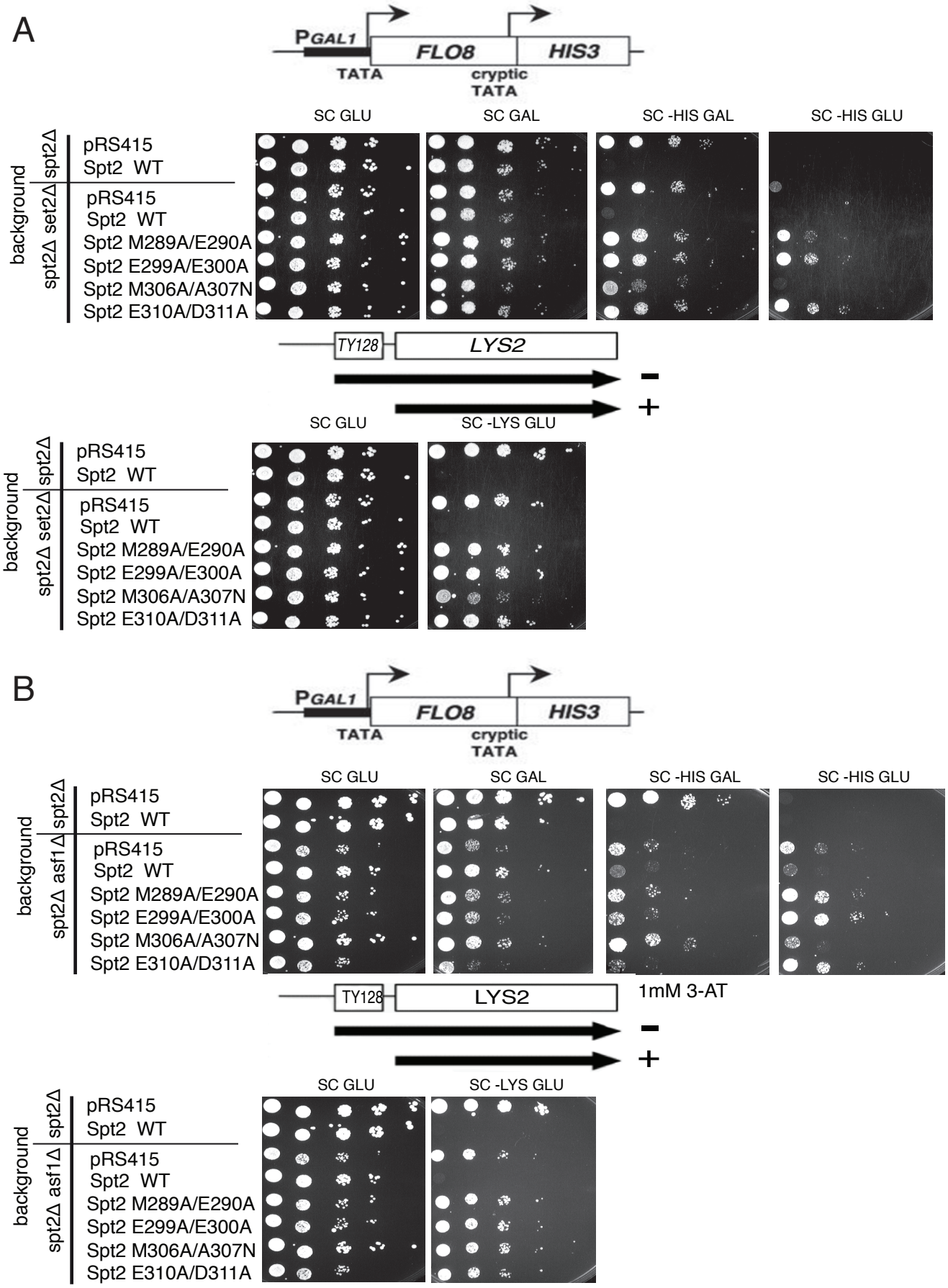

Supplemental Figure S21. *SET2* and *ASF1* deletions have no affect on the phenotypes associated with Spt2-H3/H4 mutations. Growth tests on the indicated media of *spt2Δset2Δ (A)* or *spt2Δasf1Δ (B)* cells expressing different version of Spt2 and containing the FLO8-HIS3 spurious transcription reporter or the lys2-128δ SPT reporter. Growth of these cells on –Histidine (Galactose) or –Lysine media indicate a loss of Spt2 function in the refolding of chromatin structure at transcribed regions.

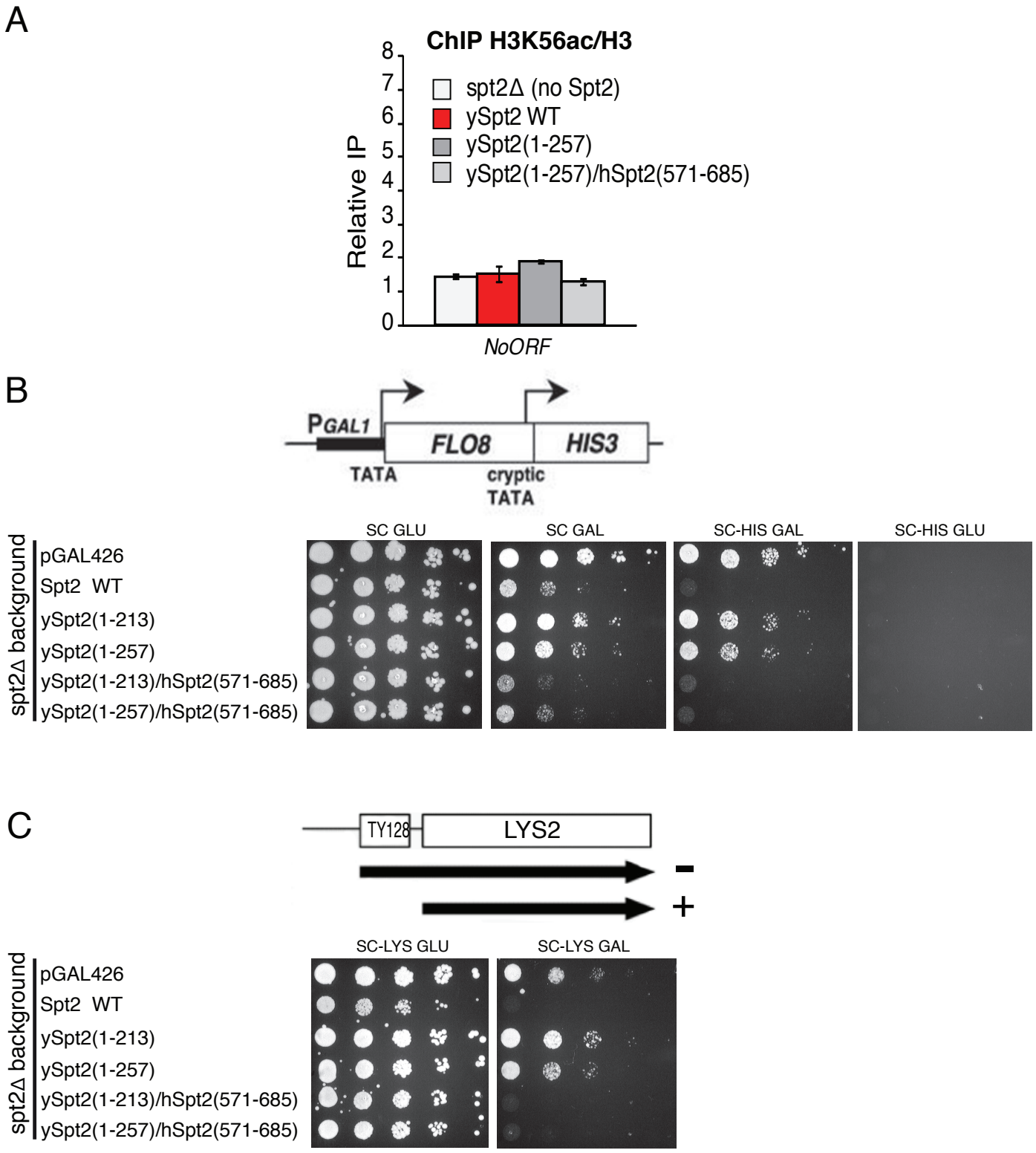

Supplemental Figure S22. Human Spt2C suppresses spurious transcription in yeast. *(A)* chromatin immunoprecipitations assessing H3K56 acetylation level at a nontranscribed loci in G1 arrested cells expressing different versions of Spt2 deleted or not in the H3/H4 interaction C-terminal domain (258-333). In contrast to active genes, human Spt2C has no effect on new H3K56ac incorporation at the non-transcribed loci NoORF (Intergenic Chr V). *(B, C)* Growth tests on the indicated media of cells expressing different versions of Spt2 fused or not to wild type and hSpt2C(571-685) and containing the FLO8-HIS3 spurious transcription reporter *(B)* or the lys2-128δ SPT reporter *(C)*. In this experiment *(B, C)*, the fusion protein was overexpressed and the resulting suppression of spt2Δ phenotypes is very efficient.

Supplementary Table S1. Crystallization trails of hSpt2C-H3/H4 complex.

Combinations	Crystals	Highest Resolution (Å)
hSpt2(571-685) + H3 (27-135) + H4	Yes	3.3 (APS)
hSpt2(579-685) + H3 (27-135) + H4	Yes	6 (BNL)
hSpt2(585-685) + H3 (27-135) + H4	Yes	4.6 (APS)
hSpt2(600-685) + H3 (27-135) + H4	Yes	10 (BNL)
hSpt2(610-685) + H3 (27-135) + H4	No	-
hSpt2(571-685) + H3 (56-135) + H4	Yes	4.2 (APS)
hSpt2(600-685) + H3 (56-135) + H4	Yes	6.5 (APS)
ySpt2(259-685) + H3 (27-135) + H4	No	-
aSpt2(591-672) + H3 (27-135) + H4	No	-

Supplementary Table S2. Data collection and refinement statistics of hSpt2C - H3/H4 tetramer complex.		
	hSpt2 (571-685)-H3/H4 tetramer	SeMet-hSpt2 (I615M)-H3/H4 tetramer
Wavelength (Å)	0.9798	0.9792
Resolution range (Å)	50 - 3.3 (3.36 - 3.3) [a]	50 - 4.60 (4.68 - 4.60) [a]
Space group	$P4_322$	$P4_322$
Cell dimensions		
a, b, c (Å)	121.2, 121.2, 118.5	128.43, 128.43, 116.89
α, β, γ (°)	90, 90, 90	90, 90, 90
Unique reflections	13827 (680)	5704 (257)
Completeness (%)	99.9 (82.4)	98.7 (88.6)
Mean I/sigma(I)	21.6 (1.1)	22.3 (1.31)
Redundancy	10.2 (10.5)	11.4 (7.8)
$R_{merge}/R_{meas}/R_{pim}$ (CC1/2)	0.093/0.098/0.038 (0.608)	0.066/0.069/0.029 (0.895)
R-work / R-free	0.24 / 0.30	-
Number of non-hydrogen atoms	2831	-
Protein	2817	-
SO_4^{2-}	5	-
H2O	9	-
RMS (bonds)	0.009	-
RMS (angles)	1.55	-
Ramachandran favored (%)	90.8	-
Ramachandran allowed (%)	9	-
Ramachandran outliers (%)	0.3	-
Wilson B-factor	51.2	-
Average B-factor	57.2	-
Protein	60.9	-
SO_4^{2-}	40.6	-

[a] Statistics for the highest-resolution shell are shown in parentheses.

Supplementary Table S3. ITC-based binding parameters for hSpt2C and ySpt2C proteins bound to histone H3(27-135)/H4 Tetramer.				
Spt2C	N value	K_d (μM)	*Δ*H (kcal/mol)	*Δ*S (cal/mol/deg)
hSpt2C (610-644)	0.88 ± 0.06	55.6 ± 4.9	-9.23 ± 0.85	-12.4
hSpt2C (637-685)	0.98 ± 0.01	2.3 ± 0.22	-38.89 ± 0.49	-109
hSpt2C (637-685), M641A	-	NDB[a]	-	-
hSpt2C (637-685), E651A/E652A	-	NDB[a]	-	-
hSpt2C (637-685), L658A/G659N	-	NDB[a]	-	-
hSpt2C (637-685), E662A/D663A	-	NDB[a]	-	-
ySpt2C (259-333)	0.89 ± 0.03	1.5 ± 0.87	-19.2 ± 0.87	-41.1
ySpt2C (282-333)	0.93 ± 0.04	10.9 ± 1.72	-7.52 ± 0.49	-2.92
ySpt2C (259-333), M289A/E290A	-	NDB[a]	-	-
ySpt2C (259-333), E299A/E300A	-	NDB[a]	-	-
ySpt2C (259-333), E310A/D311A	-	NDB[a]	-	-
ySpt2C (259-333), M306A/A307N	1.08 ± 0.01	2.1 ± 0.16	-13.43 ± 0.16	-19.9

Buffer: 500 mM NaCl, 10 mM HEPES, pH 7.5, 2 mM β-mercaptoethanol

NDB[a], no detectable binding. The standard deviation (s.d.) was derived from nonlinear fitting.

Supplementary Table S4. Saccharomyces cerevisiae strains

Strain	Genotype	Source
FY2432	*MATa ura3-52 his3Δ200 leu2Δ1 lys2-128δ* spt2Δ0::KANMX6	[Nourani et all, 2006]
YAN73	*MATa ura3-52 his3Δ200 leu2Δ1 lys2-128δ* KANMX6 pGAL-flo8::HIS3 spt2Δ0::KANMX6	This work
YPT28	*MATa his3Δ200 leu2Δ0 lys2-128δ* spt2Δ0::KANMX6 *bar1Δ::NAT ura3-52::HHF1-PGAL1/10-FLAG-HHT1-URA3*	[Thébault et all, 2011]
YAR711	*MATa ura3D0 his3Δ200 leu2Δ1 lys2-128δ* *spt2Δ0::KANMX6 bar1Δ:: KANMX6*	This work
YAR759	*MATa ura3-52 his3Δ200 leu2Δ1 lys2-128δ* KANMX6 pGAL-flo8::HIS3 spt2Δ0::KANMX6 set2Δ::KANMX6	This work
YAR769	*MATa ura3-52 his3Δ200 leu2Δ1 lys2-128δ* *KANMX6 pGAL-flo8::HIS3 spt2Δ0::KANMX6 asf1Δ::KANMX6*	This work